TISSUE ENGINEERING: Part A
Volume 15, Number 12, 2009

DOI: 10.1089/ten.tea.2009.0213

Inhibition of Histone Deacetylase Activity in Reduced Oxygen Environment Enhances the Osteogenesis of Mouse Adipose-Derived Stromal Cells

Yue Xu, M.D., Ph.D.,* Kyle E. Hammerick, B.S., M.S.,* Aaron W. James, B.A., Antoine L. Carre, M.D., Philipp Leucht, M.D., Amato J. Giaccia, Ph.D., and Michael T. Longaker, M.D., M.B.A.

Recent studies suggest that oxygen tension has a great impact on the osteogenic differentiation capacity of mesenchymal cells derived from adipose tissue: reduced oxygen impedes osteogenesis. We have found that expansion of mouse adipose-derived stromal cells (mASCs) in reduced oxygen tension (10%) results in increased cell proliferation along with induction of histone deacetylase (HDAC) activity. In this study, we utilized two HDAC inhibitors (HDACi), sodium butyrate (NaB) and valproic acid (VPA), and studied their effects on mASCs expanded in various oxygen tensions (21%, 10%, and 1% O_2). Significant growth inhibition was observed with NaB or VPA treatment in each oxygen tension. Osteogenesis was enhanced by treatment with NaB or VPA, particularly in reduced oxygen tensions (10% and 1% O_2). Conversely, adipogenesis was decreased with treatments of NaB or VPA at all oxygen tensions. Finally, NaB- or VPA-treated, reduced oxygen tension–exposed (1% O_2) ASCs were grafted into surgically created mouse tibial defects and resulted in significantly increased bone regeneration. In conclusion, HDACi significantly promote the osteogenic differentiation of mASCs exposed to reduced oxygen tension; HDACi may hold promise for future clinical applications of ASCs for skeletal regeneration.

Introduction

Skeletal defects from various causes, whether acquired or congenital, are common and clinically challenging. Current techniques for promoting the healing of bony defects are oftentimes less than ideal. Adipose-derived stromal cells (ASCs) represent a promising alternative for autologous skeletal tissue engineering.[1–4] ASCs have a demonstrated capacity for differentiation along osteogenic, chondrogenic, adipogenic, and myogenic lineages.[3] The improved utilization of ASCs, however, for the purposes of healing bony defects is dependent on biochemical or molecular cues to enhance the selection, expansion, and/or differentiation of osteoprogenitor cells within the ASC population.

Local disruption of blood supply and inflammation often occur in wounds and tissue defects, resulting in a hypoxic cellular microenvironment.[5] This hypoxic insult can prolong the wound-healing process by limiting cellular respiration, migration, and differentiation.[6–9] Hypoxia has been observed to impede successful skeletal regeneration, by impairing both osteogenesis and concomitant vasculogenesis.[5,10] Moreover, the osteogenic differentiation of ASCs and other cell types has been found to be strongly inhibited by hypoxic insult.[1,2,11,12] Previously, we demonstrated that mouse ASCs (mASCs) proliferate significantly faster in a reduced oxygen environment (2% O_2), and that the osteogenic potential of these cells is profoundly inhibited.[1,2] Increased expression of hypoxia inducible factor (HIF)-1α, a survival factor, perhaps maintains ASCs in an undifferentiated state by inhibiting the critical transcription factor *Runx2/cbfa-1*.[11,13] Strategies for overcoming hypoxic insult would be beneficial for the successful use of ASCs in skeletal repair.

Histone acetylation, in concert with other histone modifications, has been described as a major epigenetic regulator for controlling cell fate.[14,15] Histone acetyltransferases transfer acetyl groups to core histones resulting in local expansion of chromatin and increased accessibility of DNA binding proteins, leading to transcriptional activation.[16] Histone deacetylases (HDACs) counteract the activity of histone acetyltransferases, thus functioning as transcriptional repressors. These enzymes are classified into three major groups: HDACs I, II, and III.[14] Global inhibition of the

Plastic and Reconstructive Surgery Division, Hagey Pediatric Regenerative Research Laboratory, Department of Surgery, Stanford University School of Medicine, Stanford University, Stanford, California.
*These authors contributed equally to this work.

HDACs I and II groups results in growth arrest and apoptosis.[16] HDAC inhibitors (HDACi) have also been shown to regulate lineage-specific mesenchymal cell differentiation.[17–19] In particular, various HDACi are reported to enhance osteogenic differentiation in multiple cell types, including osteoblasts (OBs), bone marrow mesenchymal cells, and ASCs.[18,20–22] As reduced oxygen tension is known to alter gene transcription in part by histone modification, we hypothesized that HDACi treatment may significantly alter the cellular behavior of hypoxia-exposed ASCs.[23,24]

In this study, we first compared HDAC activity of mASCs expanded in various oxygen tensions (21%, 10%, and 1% O_2). Next, we examined the effects of two commonly used HDACi, sodium butyrate (NaB) and valproic acid (VPA), on the proliferation, osteogenic, and adipogenic differentiation of mASCs, both at atmospheric and reduced oxygen tensions (21%, 10%, and 1% O_2). Finally, we assessed the effect of transient HDACi treatment on the *in vivo* skeletal healing capacity of mASCs, through the surgical engraftment of mASCs in a murine skeletal defect.

Materials and Methods

Chemicals and supplies

Dulbecco's modified Eagle's medium (DMEM) and penicillin/streptomycin were purchased from Invitrogen (Carlsbad, CA). Fetal bovine serum (FBS) was purchased from Omega Scientific (Tarzana, CA). All cell culture wares were purchased from Corning (San Mateo, CA). Unless otherwise specified all other chemicals and supplies were purchased from Sigma-Aldrich (St. Louis, MO).

Tissue harvest and primary cell culture

mASCs were isolated from 3-week-old CD-1 mice (Charles River Laboratories, Wilmington, MA) as previously described.[1] Mouse ASCs were cultured in standard growth medium, containing DMEM, 10% FBS, and 100 IU/mL penicillin/streptomycin. ASCs were expanded for 2 days in 21%, 10%, and 1% oxygen environments, at 37°C and 5% CO_2. During expansion (i.e., for a 48-h period), mASCs were treated with NaB (1 mM), VPA (1 mM), or vehicle control (0.1% phosphate buffered saline). ASCs were subsequently harvested for assays of HDAC activity, and osteogenic and adipogenic differentiation. ASCs of passage 2 only were used, unless otherwise stated. ASCs were also isolated from mice expressing green fluorescent protein (GFP) for grafting in bone defects. Whole calvarial-derived OBs were harvested from postnatal day 5 mice as positive graft control for *in vivo* experiments.[25]

Cellular proliferation assays

Cellular proliferation was assessed by bromodeoxyuridine (BrdU) incorporation assays.[26] Briefly, mASCs were seeded in 96-well plates (1000 cells/well, $n = 6$), treated with NaB, VPA (0.5–2.0 mM), or vehicle control, and cultured at various oxygen tensions (21%, 10%, and 1% O_2). Standard growth medium supplemented with NaB or VPA (0.5–2.0 mM) was replaced every other day. After 6 days, BrdU assays were performed (Roche Applied Science, Indianapolis, IN). Means and standard deviations were calculated.

Quantitative HDAC activity assay

HDAC activity in cells was determined by Colorimetric HDAC Activity Assay Kit (BioVision, Mountain View, CA). Briefly, after 48 h of pretreatment with NaB (1 mM) or VPA (1 mM) at various oxygen tensions (21%, 10%, and 1% O_2), ASCs were lysed in a radioimmunoprecipitation buffer. Total protein content was measured by BCA protein assay kit (Pierce, Rockford, IL) according to the manufacturer's instructions. Eighty micrograms of total protein lysate was used to assay HDAC activity; assays were performed in triplicate. HDAC activity of each sample was quantitatively demonstrated as the relative optical density value normalized to microgram of total protein.

Adipogenic differentiation and assessments

Adipogenic differentiation was assessed as previously described. Cells were treated with NaB (1 mM), VPA (1 mM), or vehicle control for a 48-h period during expansion at various oxygen tensions (21%, 10%, and 1% O_2). ASCs were next seeded in 12 plates at a density of 50,000 cells/well for assessment of adipogenesis.[27] Adipogenic differentiation medium containing 10 μg/mL insulin, 1 μM dexamethasone, 0.5 mM methylxanthine, and 200 μM indomethacin, without HDACi, was added to induce adipogenesis. Adipogenic differentiation medium was changed every 3 days. Oil red O staining and quantification were performed at 1 week of differentiation.[27] Peroxisome proliferator activated receptor-γ (*PPAR-γ*) expression was examined after 1 week by quantitative real-time polymerase chain reaction (RT-PCR).

In vitro *osteogenic differentiation and assessments*

For osteogenic differentiation, cells were pretreated with NaB (1 mM), VPA (1 mM), or vehicle control for a 48-h period during expansion at various oxygen tensions (21%, 10%, and 1%). Cells were then seeded in 12-well plates (25,000 cells/well). After attachment, ASCs were treated with osteogenic differentiation medium (ODM) containing DMEM, 10% FBS, 100 μg/mL ascorbic acid, 10 mM β-glycerophosphate, and 100 IU/mL penicillin/streptomycin, in the absence of HDACi. ODM was replenished every 3 days. After 7 days, alkaline phosphatase (ALP) staining and quantification was performed as previously described.[26] All experiments were performed in triplicate; ALP positive cells appear purple. Quantification of ALP activity was determined by normalizing to the total protein quantity (Pierce).

After 14 days, alizarin red staining was performed to detect extracellular matrix mineralization.[27] To further evaluate differentiation, osteogenic-specific gene expression was examined by quantitative RT-PCR at 7-day (*Runx2*, *Col1α*, *Alp*, and *Opn*) and 14-day (*Oc*) differentiation.

RNA isolation and quantitative RT-PCR

RNA isolation was performed as previously described.[27] Briefly, isolation was performed with the RNeasy Mini Kit (Qiagen Sciences, Valencia, CA). After DNase treatment, reverse transcription was performed with TaqMan Reverse Transcription Reagents (Applied Biosystems, Foster City, CA). Quantitative RT-PCR was carried out using the Applied Biosystems Prism 7900HT Sequence Detection System and

Power Sybr Green Master Mix (Applied Biosystems). Specific primers for the genes examined were designed based on their PrimerBank (http://pga.mgh.harvard.edu/primerbank) sequence. Primer sequences are shown in Table 1. Primers were first tested to determine optimal concentrations, and products were run on a 2% agarose gel to confirm the appropriate size and RNA integrity. The levels of gene expression were determined by normalizing to the values of *GAPDH*. All reactions were performed in triplicate.

mASC healing of mouse tibial defects

Passage 1 mASCs derived from GFP transgenic mice were treated with NaB (1 mM), or VPA (1 mM), or vehicle control for 48 h during expansion at various oxygen tensions (21% and 1% O_2). Cells were then trypsinized, centrifuged, and resuspended at a concentration of 10,000 cells/μL. Passage 1 mouse OBs were also prepared at the same cell density.

All procedures were approved by the Stanford Committee on Animal Research. Skeletally mature (10–12 weeks of age) male CD-1 mice were used for this study. After anesthesia and analgesia, the right leg was shaved and cleansed. An incision was made over the proximal medial tibial diaphysis, and the anterior tibial muscle was divided until the medial surface of the tibia was exposed; great care was taken to avoid damage to the tibial periosteum. A 1-mm monocortical defect was drilled distal to the tibial tubercle using a dental drill (NSK z500; Brasseler, Savannah, GA). After irrigation, 10 μL of a cell suspension was seeded into the injury site. The tibialis anterior muscle was flipped back over the anterior surface to completely cover the defect, followed by suture adaptation. The region was irrigated and skin was closed using a nonabsorbable suture.

Tissue harvest

Mice were euthanized at postoperative day 10 to analyze early bone formation. Mice were euthanized by CO_2 inhalation and cervical dislocation. The right tibiae were harvested and fixed in 0.4% paraformaldehyde overnight. Tibiae were subjected to decalcification in 0.24 M disodium ethylenediaminetetraacetic acid and 0.24 M tetrasodium ethylenediaminetetraacetic acid water for 12 days. Tibiae were dehydrated in a gradient ethanol series, followed by paraffin embedding. Paraffin sections were cut at 8-μm thickness.

Standard histological assays

Histology was performed using a modification of the Movat's Pentachrome and Aniline Blue stains as previously described.[28,29] Pentachrome staining was used to differentiate tissue types, in which a 6% alcoholic saffron was employed to stain the collagen content of bony tissue yellow. Aniline blue staining was used to identify new osteoid matrix within the injury site, which was then analyzed by histomorphometry to quantify new bone formation.[29] For GFP immunohistochemistry, we first de-waxed sections, followed by immersion in 0.3% H_2O_2/Methanol, treatment with 0.1 M glycine and blocking in milk, bovine serum albumin, and sheep serum. Rabbit polyclonal anti-GFP primary antibody (Abcam, Cambridge, MA) was added and incubated overnight at 4°C. Sections were then washed in phosphate buffered saline, and incubated with peroxidase-conjugated secondary antibody (Jackson Immunoresearch, West Grove, PA) for 1 h at room temperature. Diaminobenzadine (VectorLab, Burlingame, CA) was used for color development.

Histomorphometry was accomplished by generating paraffin sections of the tibial injury sites. Tissues were stained with Aniline Blue; representative sections were analyzed as described below. Five animals were used for each condition. The tibial healing of injury site was represented across approximately 50 tissue sections of which 10–15 were used for histomorphometric measurements. Each section was photographed using a Leica digital imaging system (5× objective). The digital images were imported into Adobe Photoshop CS2. The region of interest typically encompassed 10^6 pixels. The number of Aniline blue–stained pixels was determined using the magic wand tool (tolerance setting; 60, histogram pixel setting; cache level 1) by a single blinded investigator, and confirmed by a second independent investigator. These data were then used to calculate the total volume of new bone formation in each injury site.[28,29]

Statistical analysis

Means and standard deviations were calculated. Statistical analysis was performed using the analysis of variance two-factor with replication when more than two groups were compared. In addition, the Welch's two-tailed *t*-test was used when standard deviations between groups were unequal. $p \leq 0.05$ was considered to be significant.

Results

NaB and VPA inhibit cellular proliferation of mASCs at various oxygen tensions

To examine the *in vitro* effects of HDACi on mASCs, cellular proliferation was first assessed by BrdU incorporation assays (Fig. 1). ASCs were cultured in three oxygen tensions, including atmospheric (21% O_2) and two reduced oxygen tensions (10% and 1% O_2) for 6 days. Culture in reduced

Table 1. Quantitative Polymerase Chain Reaction Genes and Primer Sequences

Gene name	*Forward primer sequence (5′–3′)*	*Reverse primer sequence (5′–3′)*
Alkaline phosphatase	GTTGCCAAGCTGGGAAGAACAC	CCCACCCCGCTATTCCAAAC
Type I collagen	AACCCGAGGTATGCTTGATCT	CCAGTTCTTCATTGCATTGC
Gapdh	AGGAGTATATGCCCGACGTG	TCGTCCACATCCACACTGTT
Osteocalcin	GGGAGACAACAGGGAGGAAAC	CAGGCTTCCTGCCAGTACCT
Osteopontin	AGCAAGAAACTCTTCCAAGCAA	GTGAGATTCGTCAGATTCATCCG
PPAR-γ	TCGCTGATGCACTGCCTATG	GAGAGGTCCACAGAGCTGATT
Runx2	CGGTCTCCTTCCAGGATGGT	GCTTCCGTCAGCGTCAACA

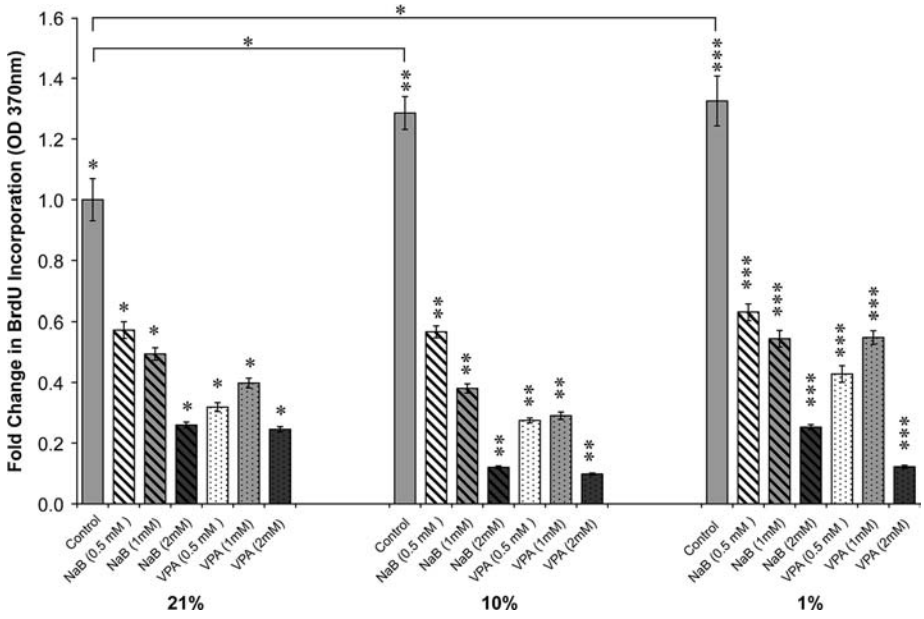

FIG. 1. Cellular proliferation at various oxygen tensions with or without histone deacetylase inhibitors (HDACi). Cellular proliferation was assayed by bromodeoxyuridine (BrdU) incorporation after 6-day growth under 21%, 10%, and 1% O_2 conditions. Hypoxia (10% and 1% oxygen) increased cellular proliferation in comparison with proliferation in normoxia (21% oxygen); see solid gray bars. Both HDACi, sodium butyrate (NaB) and valproic acid (VPA), significantly decreased BrdU uptake across all oxygen tensions (0.5–2 mM). Values are normalized to BrdU incorporation in normoxia with vehicle control; see far left. Error bars represent one standard deviation; $n = 6$, $^{*}p \leq 0.05$ versus 21% oxygen control; $^{**}p \leq 0.05$ versus 10% oxygen control; and $^{***}p \leq 0.05$ versus 1% oxygen control.

oxygen tensions (10% and 1% O_2) significantly increased BrdU incorporation, consistent with our previous observations.[1] NaB or VPA were then supplemented to medium (each at concentrations of 0.5, 1.0, and 2.0 mM). Both NaB and VPA significantly decreased BrdU incorporation in a dose-dependent manner, at all oxygen tensions.

NaB and VPA decrease HDAC activity at various oxygen tensions

To understand whether cellular proliferation was correlated with endogenous HDAC activity in mASCs, we examined HDAC activity in different oxygen conditions (Fig. 2). Interestingly, under reduced oxygen environment (10% O_2), HDAC activity was significantly increased in comparison to 21% O_2, while HDAC activity under 1% O_2 conditions did not change. As expected, both HDACi (NaB and VPA; 1 mM) were observed to decrease HDAC activity, at all oxygen tensions.

NaB and VPA decrease adipogenesis in mASCs at various oxygen tensions

To further analyze mASC differentiation potential under reduced oxygen tensions, adipogenic differentiation was examined in ASCs expanded in various oxygen tensions with or without 48-h pretreatment with NaB or VPA (1 mM) (Fig. 3). Oil red O staining demonstrated significant intracellular lipid accumulation at 21% O_2 condition by 7 days. In comparison, lipid accumulation was slightly enhanced at 10% O_2 condition,

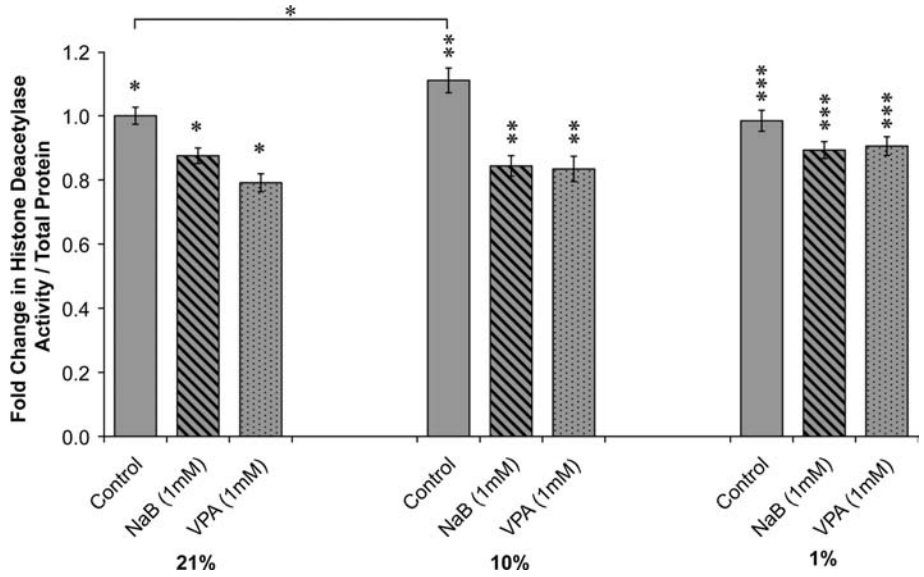

FIG. 2. HDAC activity at various oxygen tensions with or without HDACi. ASCs were expanded in 21%, 10%, and 1% oxygen conditions; HDAC activity was measured by a colorimetric reaction and normalized to total protein content. HDAC activity significantly increased at 10% O_2. Forty-eight hours of pretreatment with either NaB (1 mM) or VPA (1 mM) significantly reduced HDAC activity across all oxygen tensions. Values are normalized to control groups in 21% O_2; error bars represent the standard deviation; $n = 3$; $^{*}p \leq 0.05$ versus 21% oxygen control; $^{**}p \leq 0.05$ versus 10% oxygen control; and $^{***}p \leq 0.05$ versus 1% oxygen control.

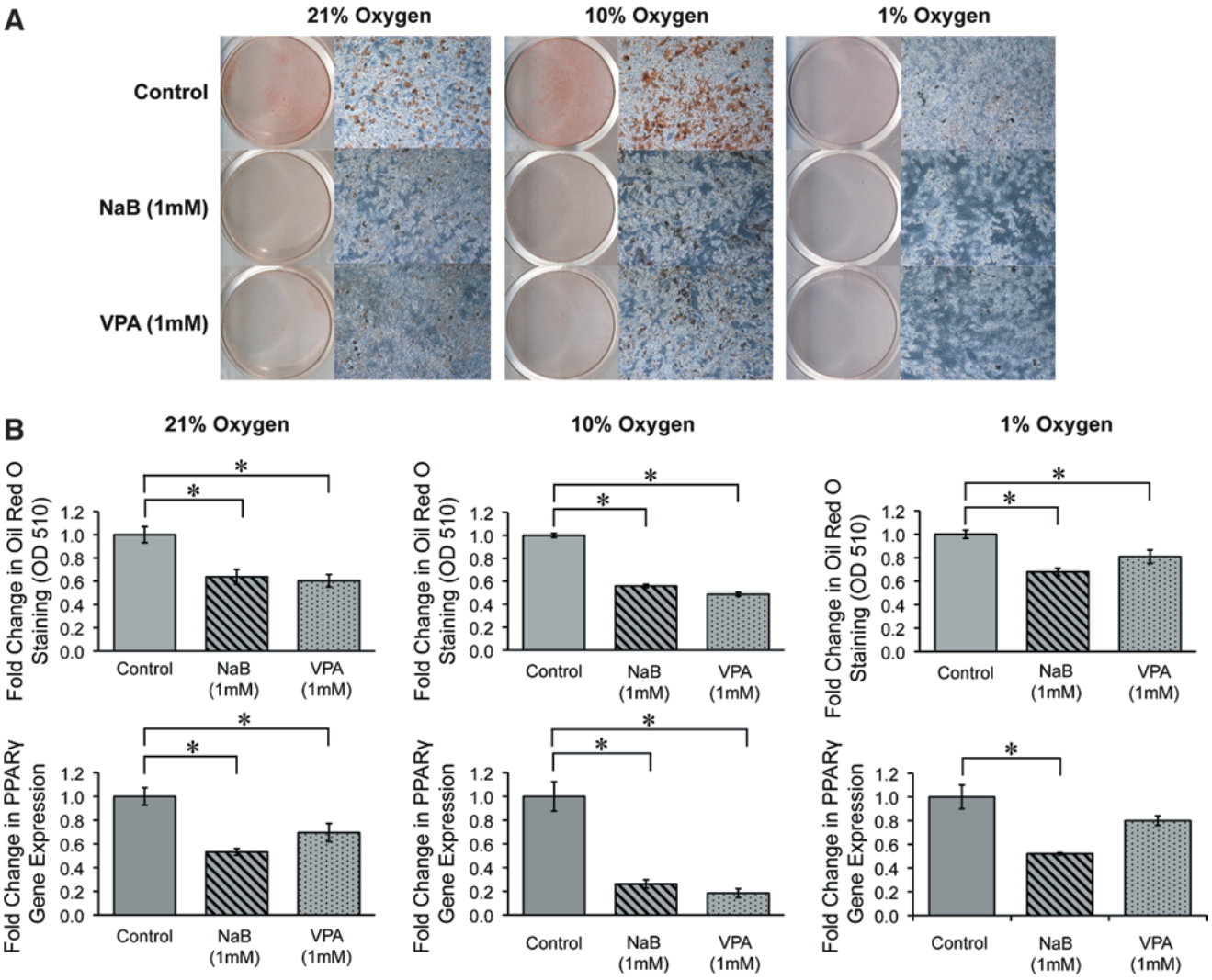

FIG. 3. Adipogenic differentiation of mouse adipose-derived stromal cells (mASCs) exposed to various oxygen tensions, with or without HDACi pretreatment. ASCs were expanded under 21%, 10%, and 1% O_2 conditions and were pretreated for 48 h with NaB (1 mM), VPA (1 mM), or vehicle as a control, followed by adipogenic induction. (**A**) Oil red O staining of intracellular lipid accumulation at 7-day differentiation. Lipid accumulation was observed in 21% and 10% O_2, while little staining was apparent at 1% O_2. HDACi-pretreated mASCs showed substantially reduced lipid at all oxygen tensions. (**B**) Top row demonstrates quantification of Oil red O staining by leaching and photometric detection. Significantly decreased staining was observed among both NaB- and VPA-pretreated ASCs. Bottom row shows *PPAR-γ* expression by quantitative real-time polymerase chain reaction. Significantly decreased gene expression in *PPAR-γ* was again observed among HDACi-pretreated ASCs. Photographs are the scanning view of whole wells and the 10× microscopical fields that represent one of the triplicate wells; values are normalized to control groups at each oxygen tension; error bars represent one standard deviation; $n = 3$; $^*p \leq 0.05$. Color images available online at www.liebertonline.com/ten.

and significantly diminished in 1% O_2 conditions (Fig. 3A). Pretreatment with NaB (1 mM) or VPA (1 mM) decreased lipid droplet formation across all oxygen tensions. Quantification of Oil red O staining by photometric measurement confirmed a significant decrease in both NaB and VPA pretreated ASCs (Fig. 3B). To confirm HDACi-mediated inhibition of adipogenic differentiation, *PPAR-γ* was examined by quantitative RT-PCR. Levels of *PPAR-γ* expression were significantly decreased with pretreatments of NaB and VPA. These results indicated that transient exposure to HDACi (NaB or VPA) suppressed the adipogenic differentiation of mASCs under 21%, 10%, and 1% O_2 conditions.

NaB and VPA enhance osteogenic differentiation of mASCs at various oxygen tensions

Next, osteogenic differentiation was examined in mASCs expanded in various oxygen tensions (21%, 10%, and 1% O_2). ASCs were pretreated with either NaB or VPA for 48 h during expansion and subsequently cultured in ODM only. ALP staining and quantification of ALP enzymatic activity were performed after 1-week differentiation in osteogenic media to assess the onset of mineralization (Fig. 4). Endogenous ALP activity was observed at all oxygen tensions (Fig. 4A). With HDACi treatment, ALP staining was

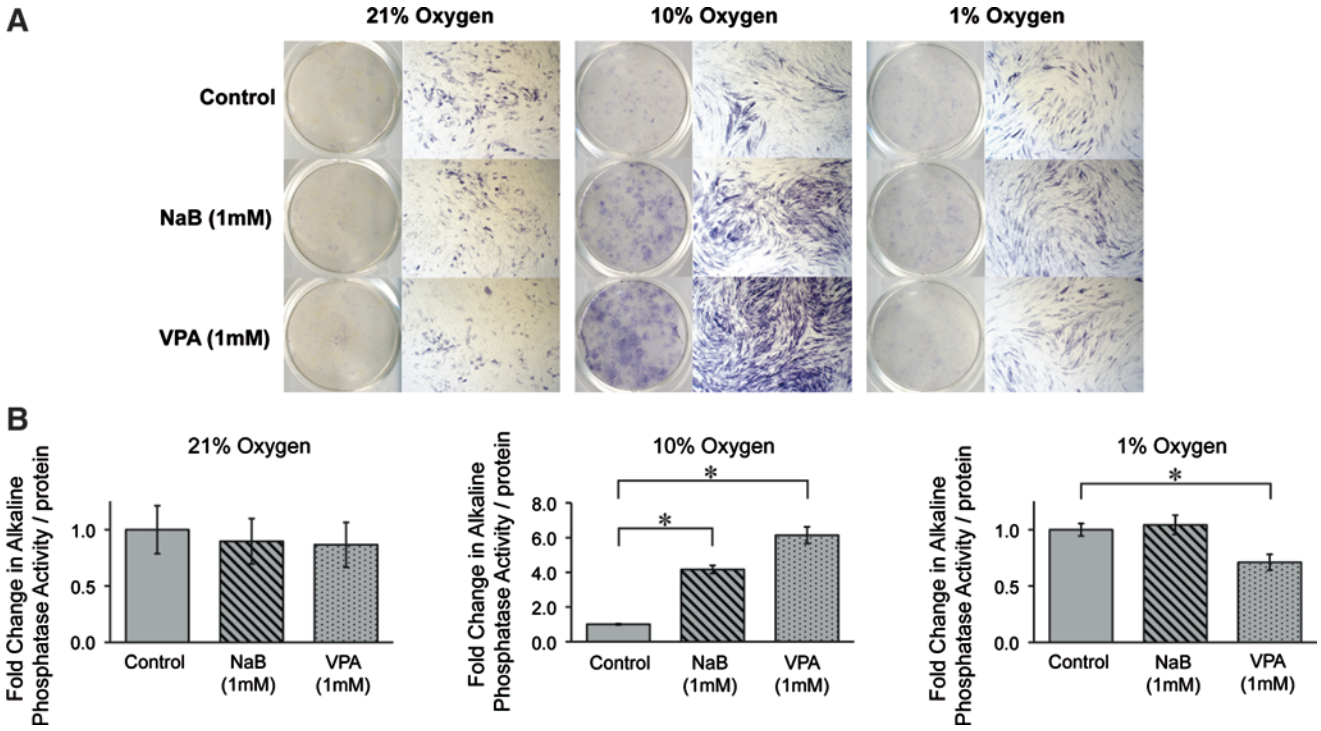

FIG. 4. Alkaline phosphatase (ALP) activity in mASCs exposed to various oxygen tensions, with or without HDACi pretreatment. ASCs were expanded under 21%, 10%, and 1% O_2 conditions and were pretreated for 48 h with NaB (1 mM), VPA (1 mM), or vehicle as a control, followed by osteogenic differentiation. (**A**) ALP staining at 1-week differentiation. Endogenous ALP staining in mASCs showed across all oxygen tensions. The intensity of staining was observed to increase among NaB- or VPA-pretreated mASCs exposed to 10% O_2. (**B**) Quantification of ALP activity normalized to total protein content after 1-week differentiation. Similar to qualitative ALP staining, enzymatic activity was increased among NaB- or VPA-treated mASCs exposed to 10% oxygen condition. Photographs are the scanning view of whole wells and 10× microscopical fields that represent one of the triplicate wells; values are normalized to control groups at each oxygen tension; error bars represent one standard deviation; $n = 3$; $^*p \leq 0.05$. Color images available online at www.liebertonline.com/ten.

significantly enhanced in 10% O_2. Quantification of ALP enzymatic activity was next assayed (Fig. 4B). Congruent with observed staining, relative ALP activity was increased approximately four and sixfold with NaB and VPA pretreatment in 10% oxygen condition. However, a similar increase was not observed at other oxygen tensions (21% and 1% O_2).

To further determine the effects of HDACi treatment on mASC osteogenic differentiation, gene expression was next assessed (Fig. 5). The master transcription factor *Runx2/Cbfa*, as well as other differentiation markers such as alkaline phosphatase (*ALP*), type I collagen (*Col I*), and osteopontin (*OPN*) were examined by quantitative RT-PCR. In 21% and 10% oxygen tensions, 48-h pretreatment with either NaB or VPA (1 mM) led to significant upregulation of nearly all gene markers examined. Under 1% O_2 conditions, NaB treatment significantly increased all gene markers, while VPA increased *Runx2/Cbfa* and *Col I* only.

Finally, terminal osteogenic differentiation of ASCs was assessed with Alizarin red staining to detect bone nodule formation, as well as osteocalcin expression, by quantitative RT-PCR at 14-day differentiation (Fig. 6). Consistent with previous results, HDACi treatment significantly enhanced bone nodule formation, as observed by increasing intensity of Alizarin red staining (Fig. 6A). This HDACi-mediated increase in bone nodule formation was most prominently observed under reduced oxygen tensions (10% and 1% O_2) (Fig. 6A). NaB or VPA treatment increased osteocalcin expression as well, at all oxygen tensions (Fig. 6B). Notably, under 1% O_2 conditions, an over 6- and 11-fold increase in expression was observed with NaB and VPA treatment, respectively.

NaB and VPA rescue in vivo *osteogenesis of mASCs exposed to reduced oxygen conditions*

Having observed that HDACi treatment significantly enhanced the osteogenic differentiation of mASCs under reduced oxygen tensions *in vitro*, we next sought to determine whether the same may hold true in an *in vivo* correlate (Fig. 7). ASCs were cultured for 48 h at various oxygen tensions (21% or 1% O_2) with NaB or VPA (1 mM); equal numbers of cells (100,000 cells in 10 μl) were grafted into a 1-mm mono-cortical mouse tibial defect (Fig 7a).[29] ASCs were derived from β-actin GFP mice so that grafted mASCs could be distinguished in a skeletal injury site. For controls, an injury was performed without cell grafting (Empty), and as a positive control, mouse calvarial-derived OBs were grafted in equal numbers.

Representative sections of defects are shown in Figure 7c retrieved after 10 days of healing *in vivo*. Sections are stained with both pentachrome, in which osteoid appears yellow (top), as well as Aniline blue, in which bone appears dark blue (bottom). For illustrative purposes, new bone formation within the defect site has been encircled with a dashed white

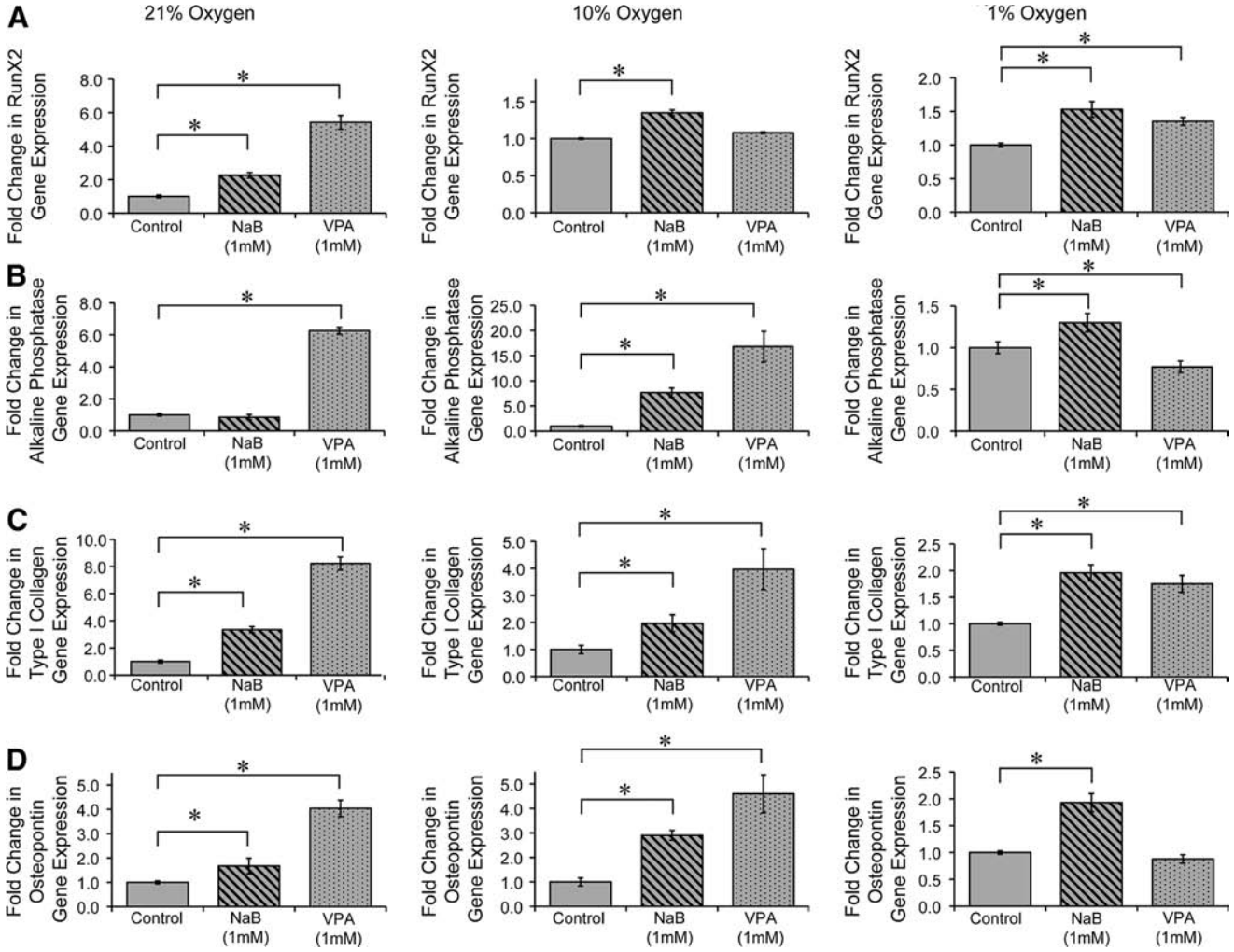

FIG. 5. Osteogenic gene expression in mASCs exposed to various oxygen tensions, with or without HDACi pretreatment. ASCs were expanded under 21%, 10%, and 1% O_2 conditions and were pretreated for 48 h with NaB (1 mM), VPA (1 mM), or vehicle as a control, followed by osteogenic differentiation. (**A**) *Runx2* gene expression after 7-day differentiation. (**B**) Alkaline phosphatase expression after 7-day differentiation. (**C**) Type I collagen expression at 7-day differentiation. (**D**) Osteopontin gene expression after 7-day differentiation. Significant enhancement of the osteogenic gene markers was observed under most conditions. Values are normalized to control groups at each oxygen tension; error bars represent one standard deviation; $n = 3$; $^*p \leq 0.05$.

line, while the edge of the defect is demarcated by a dashed black line. For each group, histomorphometric measurements of average new bone formation in the defect site were performed using Adobe Photoshop (summarized in Figure 7b). Results showed significant amounts of new trabeculated bone in defects grafted with mASCs exposed to 21% O_2 conditions (21% mASC). GFP immunostaining verified the presence of grafted cells within the defect site (data not shown). Histomorphometric measurement showed the average volume of new bone among 21% oxygen–cultured mASC-grafted defects to approximate that of OB-grafted defects. In contrast, mASCs exposed to reduced oxygen tensions (1% mASC) showed little bone regeneration upon engraftment. Histomorphometric analysis showed that new bone formation decreased in 1% oxygen–expanded mASC-grafted defects relative to empty defects: in effect grafting of mASCs exposed to reduced oxygen tensions delayed bone regeneration. However, if 1% oxygen–expanded mASCs were treated with either NaB or VPA before grafting, significantly increased bone formation was observed within the tibial injury site, verified by histomorphometric analysis. Moreover, those injury sites grafted with HDACi-pretreated, 1% oxygen–exposed mASCs showed similar bone formation as those defects grafted with 21% oxygen–exposed mASCs, verified by histomorphometry. Thus, the significant pro-osteogenic effect of transient HDACi exposure on mASCs *in vitro* was observed when cells were grafted *in vivo*.

Discussion

ASCs have recently been recognized to be a promising source for cell-based, autologous tissue regeneration.[30] Thus, understanding the cellular and molecular biology of this cell population is a current focus of translational research. Accumulating evidence suggests that local oxygen tension is a critical modulator of mesenchymal cell growth and

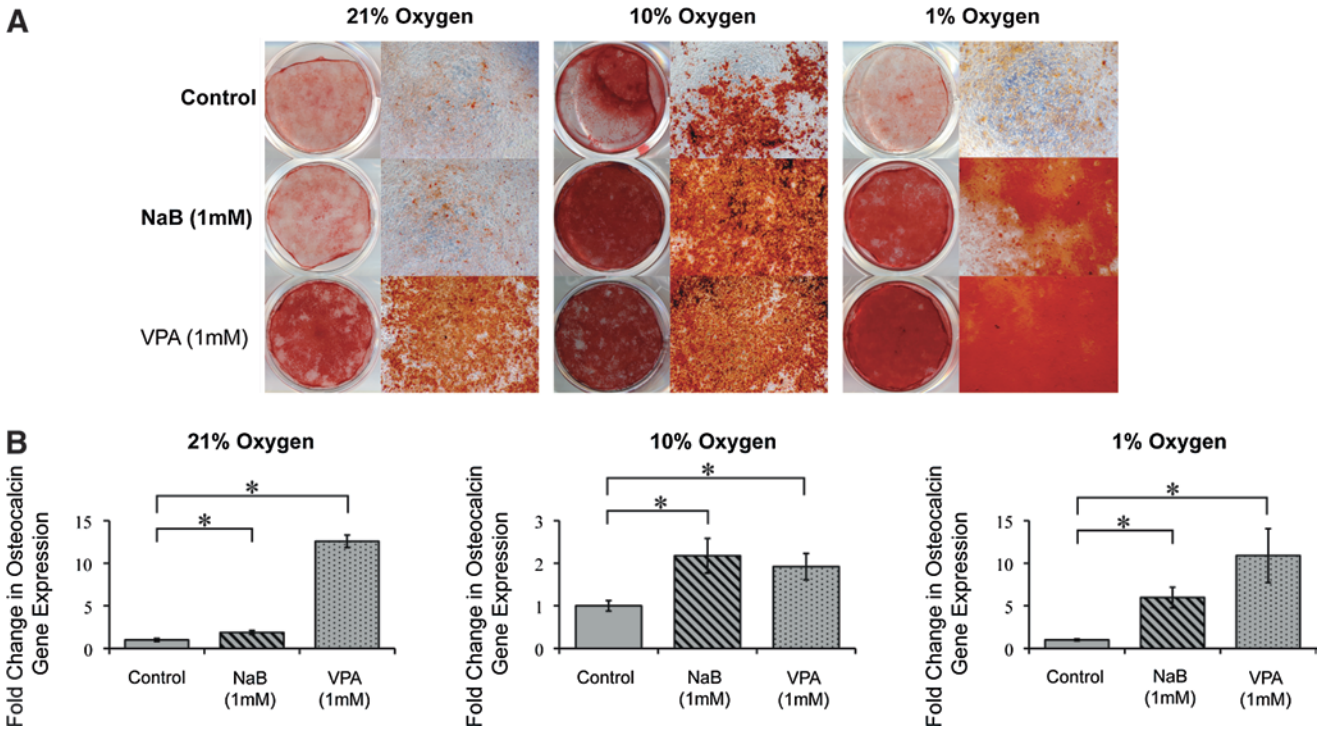

FIG. 6. Terminal osteogenic differentiation in mASCs exposed to various oxygen tensions, with or without HDACi pretreatment. ASCs were expanded under 21%, 10%, and 1% O_2 conditions and were pretreated for 48 h with NaB, VPA, or vehicle as a control, followed by osteogenic differentiation. (**A**) Alizarin red staining at 2-week differentiation. The intensity of staining was observed to increase among NaB- or VPA-pretreated ASCs, particularly those exposed to reduced oxygen tensions. (**B**) Osteocalcin gene expression by quantitative real-time polymerase chain reaction at 2-week osteogenic differentiation. Similarly, both NaB (1 mM) and VPA (1 mM) at all oxygen tensions significantly increased osteocalcin expression. Photographs are the scanning view of whole wells and 10× microscopical fields that represent one of the triplicate wells; values are normalized to control groups at each oxygen tension; error bars represent one standard deviation; $n = 3$; $^*p \leq 0.05$. Color images available online at www.liebertonline.com/ten.

differentiation.[31] Our laboratory and others have studied the effects of transient and long-term exposure to reduced oxygen tensions in osteogenic differentiation of multiple bone-forming cells, including OBs, bone marrow mesenchymal cells, and ASCs.[1,2,12,13,32] However, the cellular mechanisms through which reduced oxygen tension suppresses osteogenesis remain poorly understood. Strategies to overcome this hurdle remain unelucidated.

Runx-2/cbfa-1, an essential transcription factor for OB development and chondrocyte hypertrophy, has been shown to be significantly and persistently inhibited by transient exposure to reduced oxygen tensions.[1,2,13] This finding has important implications to the field of cell-based tissue engineering, as any type of mesenchymal stem cell transplanted *in vivo* to a hypoxic wound would likely as a consequence of having impaired bone-forming potential. HDACs are among the corepressors that interact with Runx-2.[33] HDACs and their binding proteins are complex components that influence the accessibility of regulatory elements in chromatin. In recent studies, HDAC activity has been shown to regulate the transcription of multiple osteogenic genes, including *Runx-2*, type I collagen, osteopontin, bone sialoprotein, and osteocalcin.[34,35] In addition, HIF-1, a survival factor for mesenchymal cells, plays an important role in modulating cell fate, including osteogenic and adipogenic differentiation.[36,37] Moreover, HDAC activity has been associated with HIF-dependent genes.[5,10] In this study, we demonstrated that HDAC activity was significantly induced in mASCs grown in reduced oxygen (10%) tension.

To further address changes in HDAC activity associated with mesenchymal cell differentiation, we utilized well-described HDACi (NaB and VPA) to block HDAC activity and studied the differentiation potential in mASCs expanded at various oxygen tensions (21%, 10%, and 1% O_2). We found that temporary treatment with either HDACi (NaB or VPA) after expansion in reduced oxygen tensions substantially inhibited the increased HDAC activity in these cells. Subsequently, we demonstrated increased ALP activity and enhanced cellular mineralization when mASCs were directed toward an osteogenic lineage. Further, *Runx-2* expression in HDACi-pretreated cells was shown to be elevated during osteogenic differentiation. Conversely, the adipogenic capability in these cells was suppressed with HDACi treatments. These data suggest that a tight relationship exists between HDAC activity and osteogenesis.[18] Therefore, inhibiting HDAC activity by HDACi significantly enhanced osteogenic differentiation in mASCs. In particular, when mASCs were expanded in reduced oxygen tensions we found that the temporary pretreatment with HDACi could rescue the inhibited osteogenic potentials. Interestingly, other studies

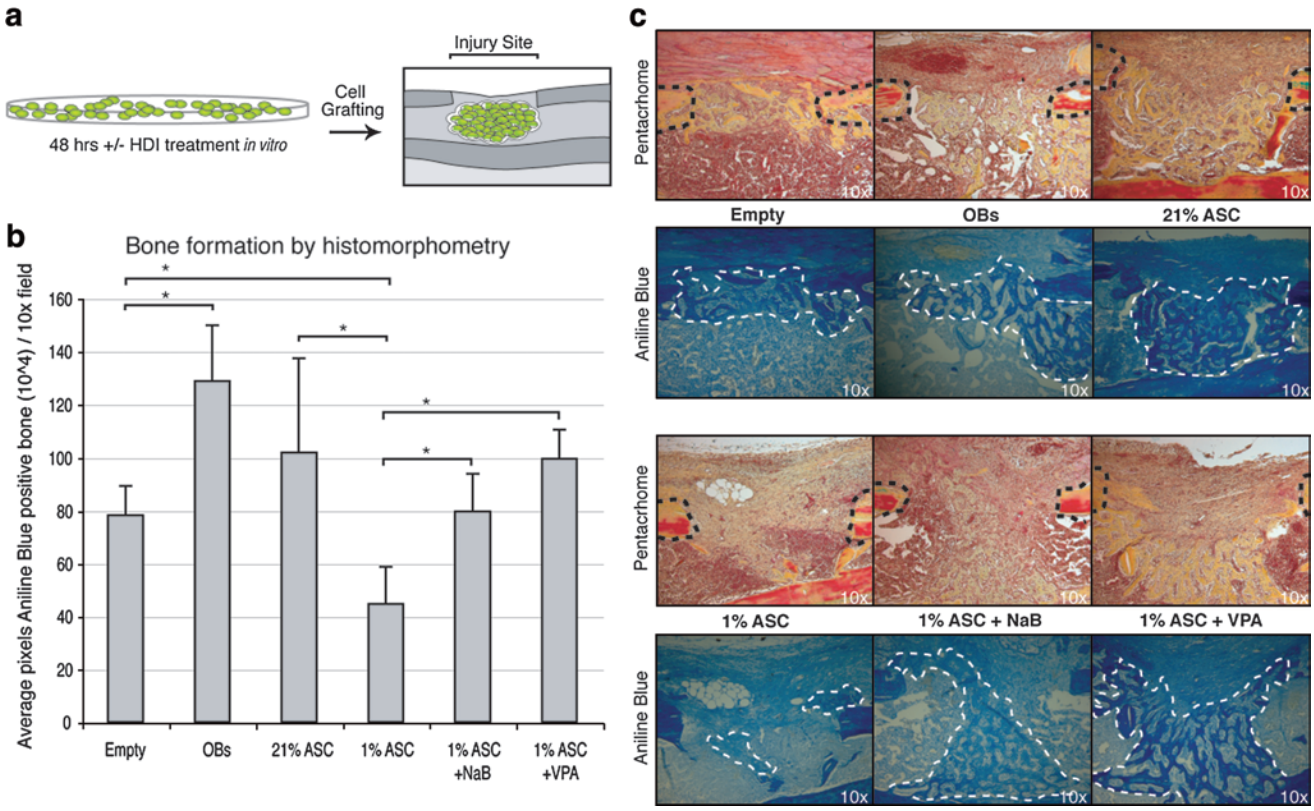

FIG. 7. Grafting of mASCs in tibial defects. (**a**) Green fluorescent protein–positive mASCs were expanded under 21% and 1% O_2 conditions with or without NaB (1 mM) or VPA (1 mM) for 48 h, followed by grafting into a mouse monocortical tibial defect. (**b**) Histomorphometric quantification of new bone formation, as pixels new bone per 10× field. (**c**) Histology of defects without grafted cells (Empty), with mouse whole-calvarial-derived osteoblasts (OBs), or mASCs expanded at 21% or 1% oxygen, with or without NaB or VPA treatment (1 mM). In Pentachrome staining, bone within the defect site appears yellow. In adjacent Aniline Blue staining, bone within the defect site appears dark blue. Dashed black lines demarcate the edges of the defect, while dashed white lines encircle new bone within the defect site. Error bars represent one standard deviation, $^*p \leq 0.05$. Color images available online at www.liebertonline.com/ten.

have also found that short pretreatment with HDACi, as opposed to continuous supplementation to ODM, significantly influences the osteogenic differentiation of other cell types.[18,35]

Effects of temporary HDACi treatments *in vitro* were also observed to have significant outcomes when mASCs were transplanted *in vivo*. Utilizing a mouse tibia defect model, we studied the osteogenic potential after *in vitro* priming of mASCs expanded in reduced oxygen tensions with HDACi. Local transplant of HDACi-pretreated cells resulted in increased new bone formation within the defect site as compared to nontreated mASC transplants. Moreover, new bone formation among injuries grafted with HDACi-pretreated, 1% oxygen–expanded cells was on par with injury sites grafted with normoxia-expanded mASCs. In contrast to our present findings, other studies have not observed an increase in osteogenesis upon *in vivo* applications of HDACi-treated mesenchymal cells.[34] It is possible that differences in species derivation (human vs. mouse), mesenchymal cell type (BMSC vs. ASC), and *in vivo* model (ectopic bone formation vs. grafting of cells into a skeletal defect) underlie this discrepancy. Thus, in summation, in this study, the deleterious effects of reduced oxygen tension on mASC osteogenic differentiation can be ameliorated by temporary exposure to HDACi. This strategy may have potential for future translational research in bone tissue regeneration.

Conclusion

Exposure to reduced oxygen tension is associated with increased HDAC activity and higher proliferation rates in mASCs. The short-term pretreatment of mASCs with HDAC inhibitors enhanced the osteogenic potential of mASCs *in vitro* and *in vivo*, and rescued the osteogenic capacity of mASCs in reduced oxygen tension. HDACi may hold promise for use in ASC-mediated skeletal tissue regeneration.

Acknowledgments

This study was supported by National Institutes of Health, National Institute of Dental and Craniofacial Research Grants R01 DE-14526 and R01 DE-13194, and the Oak Foundation to M.T.L., Hagey Foundation Fellowship to A.L.C., and Genentech Foundation Fellowship to A.W.J. We would like to thank L. MacLeod for his excellent technical assistance.

Disclosure Statement

No competing financial interests exist.

References

1. Malladi, P., Xu, Y., Chiou, M., Giaccia, A.J., and Longaker, M.T. Effect of reduced oxygen tension on chondrogenesis and osteogenesis in adipose-derived mesenchymal cells. Am J Physiol **290,** C1139, 2006.
2. Xu, Y., Malladi, P., Chiou, M., Bekerman, E., Giaccia, A.J., and Longaker, M.T. *In vitro* expansion of adipose-derived adult stromal cells in hypoxia enhances early chondrogenesis. Tissue Eng **13,** 2981, 2007.
3. Xu, Y., Malladi, P., Wagner, D.R., and Longaker, M.T. Adipose-derived mesenchymal cells as a potential cell source for skeletal regeneration. Curr Opin Mol Ther **7,** 300, 2005.
4. Zuk, P.A., Zhu, M., Ashjian, P., De Ugarte, D.A., Huang, J.I., Mizuno, H., Alfonso, Z.C., Fraser, J.K., Benhaim, P., and Hedrick, M.H. Human adipose tissue is a source of multipotent stem cells. Mol Biol Cell **13,** 4279, 2002.
5. Wang, Y., Wan, C., Deng, L., Liu, X., Cao, X., Gilbert, S.R., Bouxsein, M.L., Faugere, M.C., Guldberg, R.E., Gerstenfeld, L.C., Haase, V.H., Johnson, R.S., Schipani, E., and Clemens, T.L. The hypoxia-inducible factor alpha pathway couples angiogenesis to osteogenesis during skeletal development. J Clin Invest **117,** 1616, 2007.
6. Malda, J., Klein, T.J., and Upton, Z. The roles of hypoxia in the *in vitro* engineering of tissues. Tissue Eng **13,** 2153, 2007.
7. Wang, D.W., Fermor, B., Gimble, J.M., Awad, H.A., and Guilak, F. Influence of oxygen on the proliferation and metabolism of adipose derived adult stem cells. J Cell Physiol **204,** 184, 2005.
8. Papandreou, I., Cairns, R.A., Fontana, L., Lim, A.L., and Denko, N.C. HIF-1 mediates adaptation to hypoxia by actively downregulating mitochondrial oxygen consumption. Cell Metab **3,** 187, 2006.
9. Papandreou, I., Powell, A., Lim, A.L., and Denko, N. Cellular reaction to hypoxia: sensing and responding to an adverse environment. Mutat Res **569,** 87, 2005.
10. Wan, C., Gilbert, S.R., Wang, Y., Cao, X., Shen, X., Ramaswamy, G., Jacobsen, K.A., Alaql, Z.S., Eberhardt, A.W., Gerstenfeld, L.C., Einhorn, T.A., Deng, L., and Clemens, T.L. Activation of the hypoxia-inducible factor-1alpha pathway accelerates bone regeneration. Proc Natl Acad Sci USA **105,** 686, 2008.
11. D'Ippolito, G., Diabira, S., Howard, G.A., Roos, B.A., and Schiller, P.C. Low oxygen tension inhibits osteogenic differentiation and enhances stemness of human MIAMI cells. Bone **39,** 513, 2006.
12. Utting, J.C., Robins, S.P., Brandao-Burch, A., Orriss, I.R., Behar, J., and Arnett, T.R. Hypoxia inhibits the growth, differentiation and bone-forming capacity of rat osteoblasts. Exp Cell Res **312,** 1693, 2006.
13. Potier, E., Ferreira, E., Andriamanalijaona, R., Pujol, J.P., Oudina, K., Logeart-Avramoglou, D., and Petite, H. Hypoxia affects mesenchymal stromal cell osteogenic differentiation and angiogenic factor expression. Bone **40,** 1078, 2007.
14. Shahbazian, M.D., and Grunstein, M. Functions of site-specific histone acetylation and deacetylation. Annu Rev Biochem **76,** 75, 2007.
15. Eilertsen, K.J., Floyd, Z., and Gimble, J.M. The epigenetics of adult (somatic) stem cells. Crit Rev Eukaryot Gene Expr **18,** 189, 2008.
16. Mottet, D., and Castronovo, V. Histone deacetylases: target enzymes for cancer therapy. Clin Exp Metastasis **25,** 183, 2008.
17. Young, D.A., Lakey, R.L., Pennington, C.J., Jones, D., Kevorkian, L., Edwards, D.R., Cawston, T.E., and Clark, I.M. Histone deacetylase inhibitors modulate metalloproteinase gene expression in chondrocytes and block cartilage resorption. Arthritis Res Ther **7,** R503, 2005.
18. Cho, H.H., Park, H.T., Kim, Y.J., Bae, Y.C., Suh, K.T., and Jung, J.S. Induction of osteogenic differentiation of human mesenchymal stem cells by histone deacetylase inhibitors. J Cell Biochem **96,** 533, 2005.
19. Vega, R.B., Matsuda, K., Oh, J., Barbosa, A.C., Yang, X., Meadows, E., McAnally, J., Pomajzl, C., Shelton, J.M., Richardson, J.A., Karsenty, G., and Olson, E.N. Histone deacetylase 4 controls chondrocyte hypertrophy during skeletogenesis. Cell **119,** 555, 2004.
20. Lee, H.W., Suh, J.H., Kim, A.Y., Lee, Y.S., Park, S.Y., and Kim, J.B. Histone deacetylase 1-mediated histone modification regulates osteoblast differentiation. Mol Endocrinol **20,** 2432, 2006.
21. Jensen, E.D., Schroeder, T.M., Bailey, J., Gopalakrishnan, R., and Westendorf, J.J. Histone deacetylase 7 associates with Runx2 and represses its activity during osteoblast maturation in a deacetylation-independent manner. J Bone Miner Res **23,** 361, 2008.
22. Schroeder, T.M., Kahler, R.A., Li, X., and Westendorf, J.J. Histone deacetylase 3 interacts with runx2 to repress the osteocalcin promoter and regulate osteoblast differentiation. J Biol Chem **279,** 41998, 2004.
23. Lee, S.H., Kim, J., Kim, W.H., and Lee, Y.M. Hypoxic silencing of tumor suppressor RUNX3 by histone modification in gastric cancer cells. Oncogene **28,** 184, 2009.
24. Pluemsampant, S., Safronova, O.S., Nakahama, K., and Morita, I. Protein kinase CK2 is a key activator of histone deacetylase in hypoxia-associated tumors. Int J Cancer **122,** 333, 2008.
25. Xu, Y., Malladi, P., Zhou, D., and Longaker, M.T. Molecular and cellular characterization of mouse calvarial osteoblasts derived from neural crest and paraxial mesoderm. Plast Reconstr Surg **120,** 1783, 2007.
26. James, A.W., Xu, Y., Wang, R., and Longaker, M.T. Proliferation, osteogenic differentiation, and fgf-2 modulation of posterofrontal/sagittal suture-derived mesenchymal cells *in vitro*. Plast Reconstr Surg **122,** 53, 2008.
27. Malladi, P., Xu, Y., Chiou, M., Giaccia, A.J., and Longaker, M.T. Hypoxia inducible factor-1alpha deficiency affects chondrogenesis of adipose-derived adult stromal cells. Tissue Eng **13,** 1159, 2007.
28. Leucht, P., Kim, J.B., and Helms, J.A. Beta-catenin-dependent Wnt signaling in mandibular bone regeneration. J Bone Joint Surg **90 Suppl 1,** 3, 2008.
29. Kim, J.B., Leucht, P., Lam, K., Luppen, C., Ten Berge, D., Nusse, R., and Helms, J.A. Bone regeneration is regulated by wnt signaling. J Bone Miner Res **22,** 1913, 2007.
30. Gimble, J.M., and Guilak, F. Differentiation potential of adipose derived adult stem (ADAS) cells. Curr Top Dev Biol **58,** 137, 2003.
31. Salim, A., Nacamuli, R.P., Morgan, E.F., Giaccia, A.J., and Longaker, M.T. Transient changes in oxygen tension inhibit osteogenic differentiation and Runx2 expression in osteoblasts. J Biol Chem **279,** 40007, 2004.
32. Fehrer, C., Brunauer, R., Laschober, G., Unterluggauer, H., Reitinger, S., Kloss, F., Gully, C., Gassner, R., and Lepperdinger, G. Reduced oxygen tension attenuates differentiation capacity of human mesenchymal stem cells and prolongs their lifespan. Aging cell **6,** 745, 2007.
33. Jensen, E.D., Nair, A.K., and Westendorf, J.J. Histone deacetylase co-repressor complex control of Runx2 and bone formation. Crit Rev Eukaryot Gene Expr **17,** 187, 2007.

34. de Boer, J., Licht, R., Bongers, M., van der Klundert, T., Arends, R., and van Blitterswijk, C. Inhibition of histone acetylation as a tool in bone tissue engineering. Tissue Eng **12,** 2927, 2006.
35. Schroeder, T.M., and Westendorf, J.J. Histone deacetylase inhibitors promote osteoblast maturation. J Bone Miner Res **20,** 2254, 2005.
36. Floyd, Z.E., Kilroy, G., Wu, X., and Gimble, J.M. Effects of prolyl hydroxylase inhibitors on adipogenesis and hypoxia inducible factor 1 alpha levels under normoxic conditions. J Cell Biochem **101,** 1545, 2007.
37. Irwin, R., LaPres, J.J., Kinser, S., and McCabe, L.R. Prolyl-hydroxylase inhibition and HIF activation in osteoblasts promotes an adipocytic phenotype. J Cell Biochem **100,** 762, 2007.

Address correspondence to:
Michael T. Longaker, M.D., M.B.A.
Plastic and Reconstructive Surgery Division
Hagey Pediatric Regenerative Research Laboratory
Department of Surgery
Stanford University School of Medicine
Stanford University
257 Campus Drive
Stanford, CA 94305-5148

E-mail: longaker@stanford.edu

Received: March 31, 2009
Accepted: June 8, 2009
Online Publication Date: July 20, 2009